



doi:10.1016/j.gca.2004.04.014

## Carbonate dissolution in the guts of benthic deposit feeders: A numerical model

H. JANSEN<sup>1,\*</sup> and M. J. AHRENS<sup>2</sup><sup>1</sup>Alfred Wegener Institute for Polar and Marine Research, PO Box 12 01 61, D-27570 Bremerhaven, Germany<sup>2</sup>National Institute of Water and Atmospheric Research (NIWA), Gate 10 Silverdale Rd, P.O. Box 11-115, Hamilton, New Zealand

(Received September 3, 2003; accepted in revised form April 13, 2004.)

**Abstract**—We present a numerical model to quantify calcite dissolution in the guts of deposit feeding invertebrates. Deposit feeder guts were modeled as constantly stirred reactors (CSTRs) following terminology from digestion theory. Saturation state and dissolution of calcium carbonate were calculated from changes in total dissolved carbon dioxide and alkalinity resulting from sediment passage through the digestive tract, while accounting for dissolution of calcite and respiration of organic carbon. Typical dissolution rates for a gut volume of 1 ml ranged between 0.5–4 mg calcite d<sup>-1</sup>. Sensitivity analysis revealed gut pH, sediment organic matter (OM) content and OM reactivity to be the critical parameters determining calcite dissolution rate. Carbonate dissolution rate was inversely related to gut pH. However, calcite dissolution was found to be possible even at alkaline gut pH due to respiration by intestinal microbes. The kinetics of calcite dissolution had only marginal influence on daily calcite dissolution rates: Varying the calcite dissolution rate constant  $\kappa$  by six orders of magnitude affected calcite dissolution rates by less than a factor of 10. Calcite dissolution rates were calculated for 4 different hydrographic regimes that differed in their content of sedimentary calcite and OM and furthermore in their OM reactivity. Highest dissolution rates were calculated for the shallow water setting, where relatively high OM content facilitated high microbial respiration rates depressing gut pH. However, dissolution rates for the deep sea setting were only slightly lower, due to greatly elevated ingestion rates resulting from low OM content. As a consequence of much higher faunal abundances, shallow-water benthos is likely to contribute the vast majority of gut-mediated carbonate dissolution. Nevertheless, the fraction of sedimentary calcite that dissolves during one gut passage is probably too small to be observable by simple gravimetric analysis. This may explain the notable scarcity of evidence for gut-mediated carbonate dissolution in the literature to date. Assuming depth-dependent calcite dissolution rates and deposit feeder abundances, we estimate gut-mediated carbonate dissolution to contribute approximately 5% of the annual global sedimentary carbonate dissolution rate, which corresponds to an average calcite dissolution rate of approximately 0.5 mg m<sup>-2</sup> d<sup>-1</sup> for the entire ocean floor. Copyright © 2004 Elsevier Ltd

### 1. INTRODUCTION

Gut-mediated carbonate dissolution by sediment-ingesting marine organisms is a long-recognized, but poorly quantified diagenetic process that has received renewed interest in current efforts to quantify the magnitude of carbon flux to and from the ocean (Milliman et al., 1999). Despite considerable research over many decades, little evidence has been found confirming carbonate dissolution in deposit feeder guts (see review by Hammond, 1981). As a consequence, microbially mediated dissolution, in addition to bioturbation, burial and other transport processes, is generally considered to be the main diagenetic carbonate removal process in near-shore sediments (Aller, 1982), while chemical dissolution is assumed to predominate below the lysocline, namely at depths greater than 3000–4500 m (Milliman et al., 1999). This paper seeks to reinvestigate the role of deposit feeder digestion in sedimentary carbonate budgets using a numeric model, in order to estimate the significance of this geochemical process in different oceanographic settings.

The dissolution of calcium carbonate to bicarbonate is a pH dependent, reversible reaction with its equilibrium strongly shifted toward the bicarbonate ion under acidic conditions

(Morse and Mackenzie, 1990). Consequently, in any organism possessing a slightly acidic gut, dissolution of ingested calcium carbonate should be a common occurrence. Most deposit-feeding macrobenthos investigated to date possess slightly acidic to slightly alkaline guts, with a pH range of 5–8 (Ahrens and Lopez, 2001). In comparison, sediment pH typically ranges between 6.5–8 in limnic and coastal marine sediments (Gorham, 1960; Fisher and Matisoff, 1981), and 7.4–7.7 in deep sea sediments (Cai et al., 1995). Even though the digestive tract pH of most deposit feeders is similar or slightly lower than the surrounding sediment and exhibits a much narrower range of pH variation than terrestrial organisms (pH 2–11, Plante et al., 1990; Plante and Jumars, 1992; Withers, 1992), most deposit feeders should be capable of dissolving calcium carbonate in their guts.

The reason the evidence for carbonate dissolution in deposit feeder guts is so sparse in the literature may be a combination of magnitude and inadequate methodology: the majority of studies investigating carbonate destruction in guts, conducted several decades ago, attempted to detect carbonate dissolution by sieve analysis. This involved comparing the grain size distribution of gut contents versus that of surrounding sediments. Although reductions in grain size or mass during gut passage were indeed reported by some early researchers and attributed to carbonate dissolution (Crozier, 1918; Mayor, 1924; Emery, 1962), many other researchers employing sieve analysis were unable to detect significant evidence for this

\* Author to whom correspondence should be addressed, at Institut für Meteorologie und Klimatologie der Universität Hannover, Herrenhäuser Str. 2, D-30419, Hannover, Germany (jansen@muk.uni-hannover.de).

(Yamanouti, 1939; Yingst, 1974; Hammond, 1981). Hammond (1981) pointed out that dissolution must not necessarily entail a reduction of median grain size, since dissolution rates vary greatly between particles of different diameter and surface area, thus allowing for both an increase and decrease in median particle size. For this reason, the absence of observable grain size changes does not rule out carbonate dissolution. Hammond showed that grain size distribution of a sediment changed only minimally even when experimentally dissolving 10% of its carbonate content using strong acid. In contrast, he was able to detect minute carbonate dissolution by measuring changes in total alkalinity. By maintaining holothurians (*Holothuria mexicana*, *Isostichopus badionotus*, and *Holothuria arenicola*) digesting carbonate sediments in aquaria and monitoring alkalinity, measured changes amounted to dissolution of only 0.1–0.3% of the ingested carbonate. These fractions were one to two orders of magnitude lower than previous estimates (Mayor, 1924; Webb et al., 1977). Evidence for subtle digestive destruction of calcium carbonate was also reported by Mageau and Walker (1976), who microscopically observed chemical corrosion and etching of foraminiferal tests (in addition to physical modification and attrition) after ingestion by various deposit feeding taxa (including polychaeta, crustacea, gastropoda, asteroidea, echinoidea and holothuroidea). Emery (1962) observed a decrease in the proportion of fine to coarse grains and an increase in the proportion of insoluble material to carbonate minerals in gut contents of *Holothuria atra* sampled from mouth to anus. He interpreted this as evidence for carbonate dissolution. Jeuniaux (1969) hypothesized that the pH increase from midgut to rectum observed in some deposit feeders may be indicative of carbonate dissolution.

Marine deposit feeders process up to 25 body weights of (dry) sediment per day (Cammen, 1980) and single holothurians have been estimated to ingest between 16 kg (Crozier, 1918) and 40 kg (Bonham and Held, 1963) of sediment annually. Deposit feeders often comprise the majority of macrofauna in soft-sediment environments, which cover most of the seafloor. Hence, even if the amount of carbonate that is dissolved per gut passage is minute, the annual impact of a deposit feeding community on a sediment's carbonate budget could potentially be significant, particularly in areas lying above the lysocline with little new production or import of calcium carbonate. Furthermore, while sediment microbes generally constitute the dominant biological driving force in sediment diagenesis (Bernier, 1980, p. 81), deposit feeders may affect sediment geochemistry in a number of ways distinctly different from microbes. For example, ingestion and gut passage are likely to stress sediments mechanically, leading to attrition and compaction of particles. In addition, pore water may be extruded, absorbed or altered in composition during gut passage. Metabolites produced during the digestive process, such as organic acids, may alter pore water pH and redox conditions. Lastly, mucus and other secretions by acting as surfactants may alter the cohesiveness and other physical surface properties of the sediment and thereby affect permeability and the kinetics of dissolution or mineralization. Deposit feeders therefore represent ubiquitous biogeochemical microenvironments that, taken as a whole, could play a small but significant role in global elemental cycles.

Analogous to benthic macrofauna, many zooplanktonic or-

ganisms have diets rich in carbonate (e.g., coccolithophores, foraminifera and pteropods). Even though only a fraction of the ingested material appears to be dissolved during gut passage, biologically mediated dissolution of calcium carbonate is now believed to be the dominant carbonate removal process in the open ocean above the lysocline (Milliman et al., 1999). In a previous article, a numerical model to estimate carbonate dissolution in copepod guts calculated dissolution efficiencies as high as 15–70% when ingestion, defecation and reingestion were tightly coupled (Jansen and Wolf-Gladrow, 2001). Here we expand this model to deposit feeders ingesting carbonate sediments, in order to estimate the general magnitude of gut-mediated dissolution on the seafloor.

The current paper has three main objectives: The first is to estimate the rate of calcite dissolution in a representative deposit feeder's gut, given a variety of starting and boundary conditions. The purpose of this objective is to investigate whether gut-mediated carbonate dissolution is a likely phenomenon, and to constrain the analytical precision that would be required for measuring the process experimentally. The second objective is to test the sensitivity of our model to a variety of biological and physical factors, including gut volume, pH, sediment organic matter (OM), calcite content and dissolution kinetics, in order to identify dominant parameters. Additional questions are asked in this context: How does calcite dissolution vary between a single gut and a digestive tract consisting of several compartments? When during the digestive process does most of the calcite dissolve? What gut pH may be expected at steady state, given a set of gut dimensions and starting conditions, and how important is microbial respiration in sustaining dissolution? The third objective sets out to estimate intestinal calcite dissolution rates for different oceanographic settings, by varying key physical parameters such as water depth, sedimentary OM content and calcite content. This allows us to estimate the contribution of gut-mediated carbonate dissolution to the global sedimentary carbonate dissolution budget.

## 2. THE MODEL

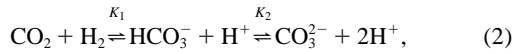
Deposit feeder intestines were modeled as constantly stirred reactors (CSTR), as classified by Penry and Jumars (1987). By placing several CSTRs in sequence, multicompartmental or plug-flow digestion could be approximated. Guts were considered to be permanently filled with sediment of homogeneous porosity. Assuming vigorous peristaltic mixing, radial concentration gradients within the gut could be neglected. For starting conditions, deposit feeders were assumed to ingest sediment of known dissolved inorganic carbon concentration and alkalinity. A variety of starting pH conditions were selected, ranging from pH 5–13. For simplification, only calcite dissolution was modeled, although other calcium carbonate minerals (e.g., aragonite) are typically encountered in natural sediments as well. Since aragonite is more soluble than calcite (Mucci et al., 1989), our model simulations present a conservative estimate of calcium carbonate dissolution in deposit feeders' guts. Effects of grain size and particle shape were parameterized via the dissolution rate constant  $\kappa$ . However, for any model run,  $\kappa$  was assumed to be invariant throughout the gut, corresponding to uniform sediment particle reactivity. Reprecipitation of carbon-

ate mineral (e.g., upon defecation) was neglected. Increases in gut pH due to calcite dissolution were countered by a respiration term producing carbon dioxide and increasing the concentration of dissolved inorganic carbon, as a result of OM respiration by gut microorganisms. This respiration rate was parameterized to depend on the reactivity of the organic carbon as a function of water depth (Middelburg, 1989).

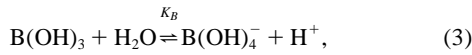
The model's independent variables are  $\text{CaCO}_3$  ( $C$ , mg) and organic carbon ( $Co$ , mg) gut content, dissolved inorganic carbon ( $D$ , mmol  $\text{mg}^{-1}$ ), alkalinity ( $A$ , mmol  $\text{mg}^{-1}$ ) and the calcium concentration ( $Ca$ , mmol  $\text{mg}^{-1}$ ). We consider carbonate alkalinity extended to include borate alkalinity and water alkalinity, which Zeebe and Wolf-Gladrow (2001, p. 34) denote as alkalinity for most practical purposes (PA). Dissolved inorganic carbon (DIC) and PA determine the carbonate system (Millero, 1995), i.e., pH and  $[\text{CO}_3^{2-}]$ , the latter being ultimately responsible for the saturation state with respect to calcite. The carbonate variables are defined as

$$\begin{aligned} \text{DIC} &= [\text{CO}_2] + [\text{HCO}_3^-] + [\text{CO}_3^{2-}], \\ \text{PA} &= [\text{HCO}_3^-] + 2[\text{CO}_3^{2-}] + [\text{B}(\text{OH})_4^-] + [\text{OH}^-] - [\text{H}^+], \\ \text{B}_T &= [\text{B}(\text{OH})_3] + [\text{B}(\text{OH})_4^-], \end{aligned} \quad (1)$$

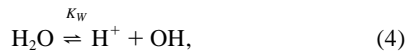
where  $\text{B}_T$  denotes the total boron concentration. The carbonate species are related by the following equilibria:



where  $K_1$  and  $K_2$  are the first and second dissociation constants of carbonic acid, respectively. The boric acid–borate equilibrium can be written as:



where  $K_B$  is the dissociation constant of boric acid. Finally, water dissociates as:



where  $K_W$  is the dissociation constant of water. The dissociation constants given by DOE (1994) were used. They have been modified depth-dependently, using the pressure corrections proposed by Millero (1995).

Given DIC and PA, the other components of the carbonate system are calculated as follows.

$$\begin{aligned} \text{DIC} \left( \frac{K_1}{[\text{H}^+]} + 2 \frac{K_1 K_2}{[\text{H}^+]^2} \right) &= \left( \text{PA} - \frac{K_B \text{B}_T}{K_B + [\text{H}^+]} - \frac{K_W}{[\text{H}^+]} + [\text{H}^+] \right) \\ &\times \left( 1 + \frac{K_1}{[\text{H}^+]} + \frac{K_1 K_2}{[\text{H}^+]^2} \right). \end{aligned} \quad (5)$$

Multiplying Eqn. 5 with  $[\text{H}^+]^3 (K_B + [\text{H}^+])$  yields an equation of fifth order for  $\text{H}^+$ , i.e., pH. Once pH is determined, one can calculate  $[\text{CO}_3^{2-}]$  as

$$[\text{CO}_3^{2-}] = \frac{\text{DIC} K_1 K_2}{[\text{H}^+]^2 + K_1 [\text{H}^+] + K_1 K_2}. \quad (6)$$

The model's equations are as follows. The deposit feeder's gut

is assumed to consist of  $N$  compartments. For the first compartment, we have

$$\begin{aligned} \frac{dC_1(t)}{dt} &= \alpha I_t - (f_1(t) + \tilde{K}) C_1(t), \\ \frac{dCo_1(t)}{dt} &= \frac{1}{2} \beta I_t - (k + \tilde{K}) Co_1(t), \\ \frac{dD_1(t)}{dt} &= \frac{\gamma(D_{bulk} - D_1(t)) + f_1(t) C_1(t)/100 + k Co_1(t)/12}{\rho_w V_1(t)}, \\ \frac{dA_1(t)}{dt} &= \frac{\gamma(A_{bulk} - A_1(t)) + 2f_1(t) C_1(t)/100}{\rho_w V_1(t)}, \\ \frac{dCa_1(t)}{dt} &= \frac{\gamma(Ca_{bulk} - Ca_1(t)) + f_1(t) C_1(t)/100}{\rho_w V_1(t)}, \end{aligned} \quad (7)$$

where  $I_t$  ( $\text{mg d}^{-1}$ ) denotes the ingestion rate of total sediment and  $\alpha$ ,  $\beta$  the fraction of sediment that is calcium carbonate and OM, respectively, where we assume 50% of the OM to be carbon (hence the factor 1/2). The respiration rate constant of organic carbon is denoted by  $k$  ( $\text{d}^{-1}$ ) and  $Co_1(t)/12$  is organic carbon converted to mmol.  $\rho_w$  ( $\text{mg mm}^{-3}$ ) is the density of seawater,  $K$  ( $\text{d}^{-1}$ ) is the gut clearance rate and  $\tilde{K} = NK$ , as all compartments have the same volume.  $\gamma$  ( $\text{mg d}^{-1}$ ) is the uptake rate of sediment pore water.  $f(t)$  ( $\text{d}^{-1}$ ) denotes the fraction of carbonate dissolving per day at time  $t$ .  $C_1(t)/100$  is the amount of calcite in the first gut compartment, converted to mmol. DIC and alkalinity of bulk pore water are given by  $D_{bulk}$  and  $A_{bulk}$ , respectively. The effective gut compartment volume, i.e. total volume minus particulate contents is denoted by  $V_1(t) = V/N - \text{solid contents}$  ( $\text{mm}^3$ ).

For subsequent gut compartments, we have

$$\begin{aligned} \frac{dC_i(t)}{dt} &= \tilde{K} C_{i-1}(t) - (f_i(t) + \tilde{K}) C_i(t), \\ \frac{dCo_i(t)}{dt} &= \tilde{K} Co_{i-1}(t) - (k + \tilde{K}) Co_i(t), \\ \frac{dD_i(t)}{dt} &= \frac{\gamma(D_{i-1}(t) - D_i(t)) + f_i(t) C_i(t)/100 + k Co_i(t)/12}{\rho_w V_i(t)}, \\ \frac{dA_i(t)}{dt} &= \frac{\gamma(A_{i-1}(t) - A_i(t)) + 2f_i(t) C_i(t)/100}{\rho_w V_i(t)}, \\ \frac{dCa_i(t)}{dt} &= \frac{\gamma(Ca_{i-1}(t) - Ca_i(t)) + f_i(t) C_i(t)/100}{\rho_w V_i(t)}, \end{aligned} \quad (8)$$

with  $i = 2, \dots, N$ .

The uptake rate of sediment pore water is derived as

$$\gamma = \frac{\phi \rho_w}{1 - \phi \rho_s} I_t, \quad (9)$$

where  $\phi$  ( $-$ ) is the porosity of sediment and  $\rho_s$  ( $\text{mg mm}^{-3}$ ) denotes sediment density. The carbonate dissolution rate is modeled according to Keir (1980). It depends on the degree of calcite undersaturation in the gut via

Table 1. Parameters of the deposit feeder model.

Parameter, symbol	Range (standard value)	Reference
Gut volume, $V$	$10^{-1}$ – $10^4$ mm <sup>3</sup> (1000 mm <sup>3</sup> , 10 mm <sup>3</sup> ) <sup>a</sup>	Penry and Jumars (1990)
CaCO <sub>3</sub> sediment fraction, $\alpha$	0–0.9 (0.1)	—
OM sediment fraction, $\beta$	0–0.6 (0.02)	—
C <sub>org</sub> respiration rate, $k$	0.0001–0.1 d <sup>-1</sup> (0.025 d <sup>-1</sup> )	Middelburg (1989)
–log[H <sup>+</sup> ], pH	5.5–7.5 (–)	Ahrens and Lopez (2001)
sediment porosity, $\phi$	– (0.8)	Berner (1980)
calcite density, $\rho_c$	– (2.7 mg mm <sup>-3</sup> )	Young (1994)
clay density, $\rho_{cl}$	– (2.65 mg mm <sup>-3</sup> )	Grim (1962)
OM density, $\rho_o$	– (1.07 mg mm <sup>-3</sup> ) <sup>b</sup>	Young (1994)
sea water density, $\rho_w$	1.02–1.06 mg mm <sup>-3</sup> (1.04 mg mm <sup>-3</sup> ) <sup>c</sup>	—
sediment density, $\rho_s$	– (2.63 mg mm <sup>-3</sup> ) <sup>d</sup>	—
gut compartments, $N$	1–30 (3)	—

<sup>a</sup> “Large gut” and “small gut” case, respectively.

<sup>b</sup> Assuming the sediment to be dominated by clay.

<sup>c</sup> Value at 3000 m depth,  $T = 2^\circ C$  and  $S = 35$ .

<sup>d</sup> Assuming that sediment is 2% OM, 20% calcite and 78% clay.

$$f(t) = \begin{cases} \kappa (1 - \Omega(t))^\eta & \text{if } \Omega(t) < 1, \\ 0 & \text{if } \Omega(t) \geq 1, \end{cases} \quad (10)$$

with  $\kappa$ (d<sup>-1</sup>) being the dissolution rate constant and  $\eta$  is the dissolution rate order.  $(1 - \Omega)$  denotes the degree of calcite undersaturation with the saturation state  $\Omega$  given as

$$\Omega = \frac{[\text{CO}_3^{2-}][\text{Ca}^{2+}]}{K_{sp}}, \quad (11)$$

where  $K_{sp}$  (mmol<sup>2</sup> mg<sup>-2</sup>) is the solubility product of calcite, which, along with its depth dependent pressure correction, is taken from Millero (1995). The key biological parameters, ingestion rate and gut passage time, are parameterized to be functions of body mass and the fraction of sedimentary OM. Ingestion rate of total sediment ( $I_t$ , mg d<sup>-1</sup>) is scaled to body dry mass ( $W_d$ , mg) as (Cammen, 1980)

$$I_t = \frac{0.453 W_d^{0.77}}{\beta^{0.92}}, \quad (12)$$

where  $\beta$  is the sediment fraction present as OM. As is apparent, the ingestion rate decreases with increasing OM proportion. To obtain a relationship between body mass and gut volume, several assumptions have to be made. First, body dry mass is considered to be 20% of body wet mass (corresponding to 80% of the organism being water). The mean density of the organism is assumed to be  $\rho = 1.1$  mg mm<sup>-3</sup> (unpublished personal observation). Assuming further the volume of the organism to

be 3.2-fold the gut volume (median of 33 deposit-feeding polychaete species, as determined by Penry and Jumars, 1990) yields the following:

$$V = \frac{5 W_d}{3.2 \rho} = 1.42 W_d \quad (13)$$

Thus, ingestion rate relates to gut volume as

$$I_t = \frac{0.35 V^{0.77}}{\beta^{0.92}}. \quad (14)$$

Gut passage time is the inverse of the gut clearance rate  $K$  (d<sup>-1</sup>). It is defined as the ratio of gut volume (assuming complete and constant gut fullness) and ingestion rate on a volume basis. To convert mass ingestion as defined in Eqn. 14 to volume ingestion  $I_{t,v}$  (mm<sup>3</sup> d<sup>-1</sup>), we consider the porosity and density of the sediment:

$$I_{t,v} = \frac{I_t}{\phi \rho_w + (1 - \phi) \rho_s}. \quad (15)$$

Thus, gut passage time is parameterized as

$$K^{-1} = \frac{V}{I_{t,v}} = 2.9 [\phi \rho_w + (1 - \phi) \rho_s] V^{0.23} \beta^{0.92}. \quad (16)$$

Standard parameter values are given in Tables 1 and 2. The default choice of gut volume ( $V = 1000$  mm<sup>3</sup>, 10 mm<sup>3</sup> for a

Table 2. Carbonate system parameters.

Parameter, symbol	Range (standard value)	Reference
CaCO <sub>3</sub> dissolution rate constant, $\kappa$	0.0025–30 d <sup>-1</sup> (5 d <sup>-1</sup> )	Keir (1980); Aller (1982)
CaCO <sub>3</sub> dissolution rate order, $\eta$	1–5 (4.5)	Keir (1980)
Bulk pore water DIC, $D_{bulk}$	$2 \cdot 10^{-6}$ – $3.5 \cdot 10^{-6}$ mmol mg <sup>-1</sup> ( $3.0 \cdot 10^{-6}$ ) <sup>a</sup>	Sayles (1980)
Bulk pore water alkalinity, $A_{bulk}$	$2.5 \cdot 10^{-6}$ – $3.0 \cdot 10^{-6}$ mmol mg <sup>-1</sup> (–) <sup>b</sup>	Sayles (1980)
Bulk pore water calcium concentration, $Ca_{bulk}$	– ( $10.28 \cdot 10^{-6}$ mmol mg <sup>-1</sup> )	Millero (1982)

<sup>a</sup> Value at 3000 m depth.

<sup>b</sup> Adjusted to yield desired initial pH.

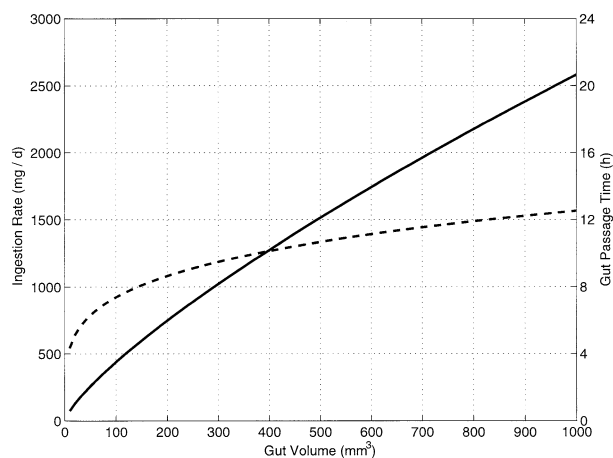


Fig. 1. Influence of gut volume on sediment ingestion rate (solid line) and gut passage (dashed line), for a sediment organic matter content of 0.02.

large and small gut example, respectively, as estimated from Penry and Jumars, 1990) and OM sediment fraction ( $\beta = 0.02$ ) yields

$$\begin{aligned} I_i &= 2613 \text{ mg d}^{-1}, 75 \text{ mg d}^{-1}, \\ K^{-1} &= 12.7 \text{ h}, 4.4 \text{ h}, \end{aligned} \quad (17)$$

for the large and small gut case, respectively. The ingestion rate and gut passage time for the whole parameter range are illustrated in Figure 1.

### 3. RESULTS

#### 3.1. Standard Model Run

As standard model cases, we define four hydrographic regimes that differ in pressure and the reactivity of their sedimentary organic matter (Table 3). Within the four basic regimes, we define subregimes with typical values of OM and calcite content. Guts were modeled to consist of three compartments with a total volume of  $1000 \text{ mm}^3$  (large gut case) and  $10 \text{ mm}^3$  (small gut case). Results for the various subregimes are presented in Table 4. Over the four hydrographic regimes, calcite dissolution rates ranged between  $0.5$  and  $4.4 \text{ mg d}^{-1}$ . Highest absolute dissolution rates were calculated for the shallow water regime with its high OM content and high OM reactivity. Steady-state gut pH ranged between 5.2 and 7.6. Figures 2 and 3 display a model run with standard parameters from Tables 1 and 2 for the shelf regime and the large gut case. Note the rapid rise in saturation state  $\Omega$  to 0.7–0.8 within 3 hours of ingestion. Midgut and hindgut compartments dissolved more calcite than the foregut, evidenced by greater changes in pH,  $\Omega$ , DIC and alkalinity.

#### 3.2. Sensitivity Studies

In the following section, we describe sensitivity studies with respect to starting gut pH, choice of sediment and kinetic parameters, gut volume and number of gut compartments.

##### 3.2.1. Starting Gut pH

Starting gut pH had a noticeable influence on calcite dissolution efficiency and the absolute dissolution rate: as illustrated in Figure 4, a lower starting gut pH led to more dissolved calcite. Depending on the hydrographic regime (i.e., calcite and OM content) a decrease of starting pH from 7 to 5 increased calcite dissolution from  $0.1$ – $8.5 \text{ mg d}^{-1}$ . Below pH 6, the deep sea setting had the highest dissolution rate due to high ingestion rates as a result of low OM content. For  $\text{pH} > 6.5$ , the shallow water settings dissolved the most calcite, as a result of high organic matter reactivity and correspondingly high respiration rates, which counteracted pH rises. Thus, the high OM content of sewage sediment allowed calcite dissolution to occur at a higher pH than in coralline sediment, even though the absolute dissolution rate was lower (Table 4). The deep sea case displayed noticeably more variability in calcite dissolution when pH is altered than the shallow water regime, yet calcite dissolution was unaffected by the fraction of sedimentary calcite. Calcite dissolution for the shelf scenario showed intermediate dependence on starting gut pH. As for the shallow water scenarios, higher OM content allowed more calcite dissolution at higher pH values: due to the strong coupling of OM content and respiration rate, dissolution is able to proceed for a starting pH as high as 12.25 in the high OM case, while it ceased beyond pH 9.25 under normal, OM-poor, shelf conditions. As visible from Figure 4 from the intersection of the calcite dissolution plots with the x-axis, the theoretical starting gut pH at which dissolution ceases, lies between approximately pH 7.5–7.75 for the deep sea and continental rise, pH 9.25 for normal (OM-poor) shelf sediment, and around pH 12.5–13.25 for the shallow and upwelling shelf cases, reflecting primarily differences in OM content and reactivity between these oceanographic settings. However, these thresholds are purely hypothetical, since in most cases sediment and gut pH will not exceed pH 9.

##### 3.2.2. Model Simulations with Fixed pH

Alternatively, we considered the case where the gut pH is completely controlled by the organism and thus fixed to the initial value. We repeated the standard run under this presumption. Results are illustrated in Figures 5 and 6. Dissolution rates were significantly higher with fixed pH compared to variable pH. For the normal shelf regime,  $4.1 \text{ mg d}^{-1}$  calcite were dissolved when pH was fixed to 6.5, while with variable pH only  $1 \text{ mg d}^{-1}$  calcite was dissolved (Table 4).

##### 3.2.3. Number of Gut Compartments

We also investigated the influence of the number of gut compartments to test whether placing several guts in sequence increases dissolution efficiency. Figure 7 displays the depen-

Table 3. Model benthic regimes.

Regime	Water depth (m)	Apparent age $C_{\text{org}}$ (d)	$C_{\text{org}}$ decay rate $k$ ( $\text{d}^{-1}$ )
Shallow water	20	~1	0.1
Shelf	200	13	0.01
Continental rise	1000	148	0.001
Deep sea	4000	1672	0.0001

Table 4. Results for selected subregimes, large gut. Starting gut pH is set to 6.5.

Regime and subregime	Calcite (frac.) <sup>a</sup>	OM (frac.) <sup>b</sup>	Calcite dissolution (mg d <sup>-1</sup> )	Steady-state gut pH
<i>Shallow water</i>				
Mud	0.01	0.06	3.3	5.62–5.82
Shell-hash	0.1	0.06	3.8	5.68–5.91
Coralline	0.9	0.02	4.4	6.25–6.52
Sewage	0.01	0.2	2.1	5.21–5.40
<i>Shelf</i>				
Normal	0.1	0.02	1.0	6.90–7.06
Upwelling	0.1	0.2	1.4	5.72–5.97
<i>Continental rise</i>				
Normal	0.2	0.01	0.5	7.29–7.34
<i>Deep sea</i>				
Clay	0.1	0.002	2.1	7.44–7.56
Diatom ooze	0.03	0.002	2.1	7.37–7.53
Foraminiferal ooze	0.6	0.002	2.1	7.51–7.58

<sup>a</sup> Estimated from Dietrich et al. (1975).

<sup>b</sup> Estimated from Reimers (1982) and Bezrukov et al. (1977).

gency for the standard shelf case (Table 3). Dissolution efficiency initially increased with additional compartments but levelled out at five compartments. However, even with three compartments, as used in the standard model runs, dissolution efficiency was the same as for more compartments when rounded to two digits.

### 3.2.4. Calcite Dissolution Kinetics

Up to now, we have used the calcite dissolution kinetic parameterization proposed by Keir (1980). However, the choice of  $\kappa$  and  $\eta$  in Eqn. 10 is but one of many possible. In order to test the model's sensitivity to dissolution kinetics,

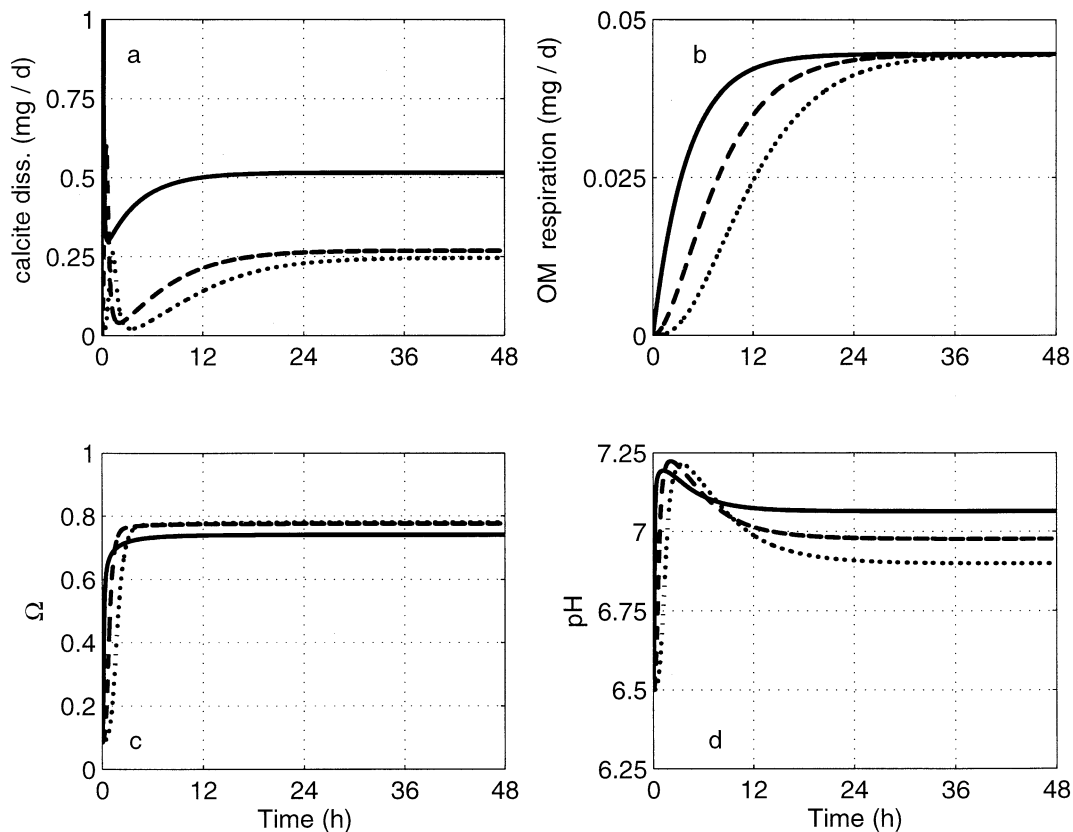


Fig. 2. Evolution of dissolution processes within a deposit feeder's gut (1 mL volume, standard shelf conditions), for three gut compartments, fore gut (solid line), mid gut (dashed-line) and hind gut (dotted line). (a) Calcite dissolution rate. (b) OM respiration rate. (c) Calcite saturation ( $\Omega$ ). (d) Gut pH. Calcite dissolution rate in the fore gut initially peaks at  $\approx 2.5$  mg d<sup>-1</sup> (data not shown).

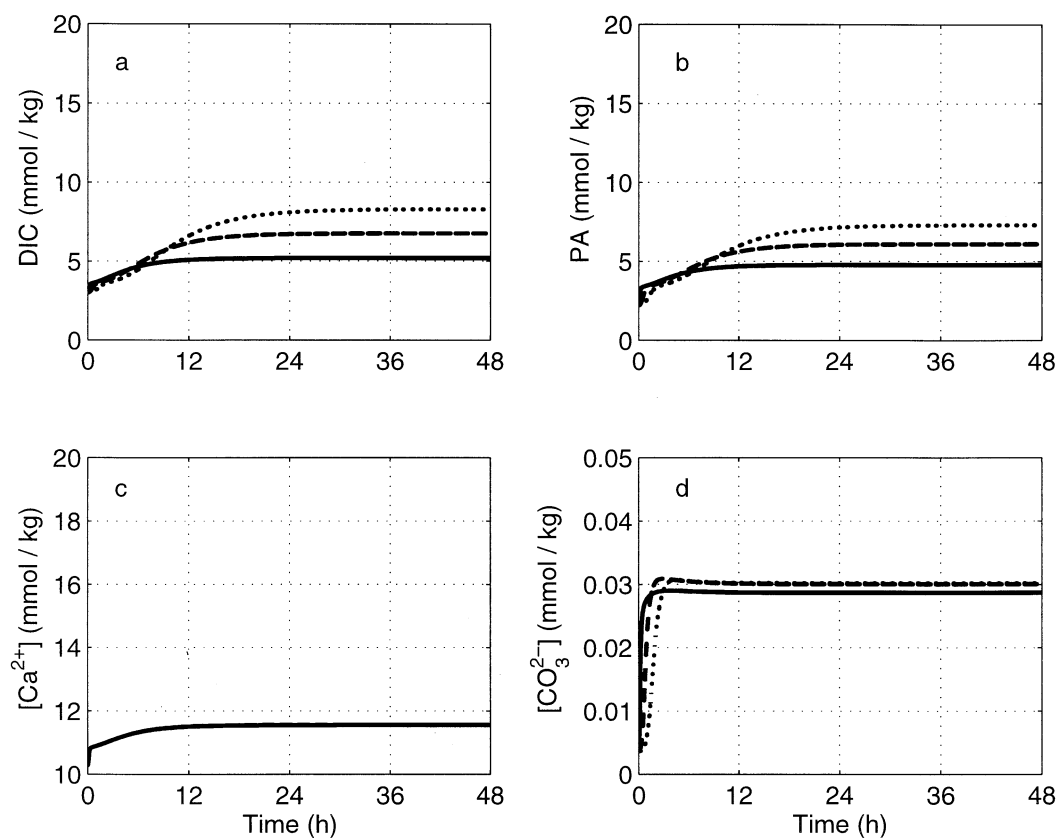


Fig. 3. Fate of dissolved substances in a deposit feeder's gut (1 mL volume, standard shelf conditions), for three gut regions, fore gut (solid line), mid gut (dashed line) and hind gut (dotted line). (a) Dissolved inorganic carbon (DIC). (b) Alkalinity (PA). (c) Dissolved  $\text{Ca}^{2+}$ . (d) Dissolved carbonate.

model runs were performed for all subregimes presented in Table 4 with five choices of parameterization (Table 5). As illustrated in Figure 8, calcite dissolution rates were not very sensitive to the assumed calcite dissolution kinetics. Although in case 5,  $\kappa$  was three orders of magnitude lower than in case 1 (our default choice), calcite dissolution was only by a factor of 2 lower with Aller's (1982) parameterization compared to the one of Keir (1980). Other parameterizations rendered even smaller differences, and increasing  $\kappa$  to  $1000 \text{ d}^{-1}$  increased dissolution by less than 20% (results not shown). With such high calcite reactivity, there is practically no kinetic hindrance to calcite dissolution, thus calcite dissolution rate is essentially limited by thermodynamics alone (i.e., the degree of carbonate undersaturation). Calcite reactivity becomes increasingly important for small values of  $\kappa_1$  where together with calcite content ( $\alpha$ ),  $\kappa$  determines the size of the calcite "stock" that is able to dissolve per unit time. For this reason, hydrographic settings with a high calcite content, such as shallow coralline sediments or deep sea foram oozes, display relatively higher dissolution efficiencies under slow kinetics than comparable regimes with lower calcite content.

### 3.2.5. Sedimentary Calcite and OM Content

Next, the effect of varying the sediment fractions of calcite ( $\alpha$ ) and OM ( $\beta$ ) was investigated. Table 4 and Figure 9 sum-

marize the results for the four different hydrographic regimes, using the standard values from Tables 1 and 2 and organic carbon decay rates from Table 3. We found  $\beta$  to have a much greater influence on calcite dissolution than  $\alpha$ . This reflected the central role of OM in the model: Sediment ingestion rate and gut passage time are, by definition, dependent on OM alone (Eqns. 14 and 16). Furthermore, the steady-state pH also depends mainly on the fraction and reactivity of OM, since these parameters together determine the magnitude of respiration by intestinal microbes. Since respiration is positively correlated with OM content, which is inversely correlated with ingestion rate (cf. Eqn. 14), one can expect an intermediate value of  $\beta$ , for which calcite dissolution attains a maximum. For example, for the shallow water and shelf settings, calcite dissolution rates peaked at an OM content of  $\sim 2\%$  and  $\sim 10\%$ , respectively (Fig. 9a, b). Dissolution rates diminished at OM values above the respective optimum due to a depression of ingestion rates, and similarly, calcite dissolution rates rapidly decreased below 2% or 10% by reduced microbial respiration. The location of the maximum within the spectrum of sediment OM values (i.e.,  $\beta$ ) depends on OM reactivity ( $k$ ): A higher value of  $k$  leads to greater respiration for a given value of  $\beta$ , and thus lowers the  $\beta$  at which calcite dissolution rate reaches a maximum. Thus, calcite dissolution rate peaks at a lower OM value for the shallow water setting than for the shelf scenario as a conse-

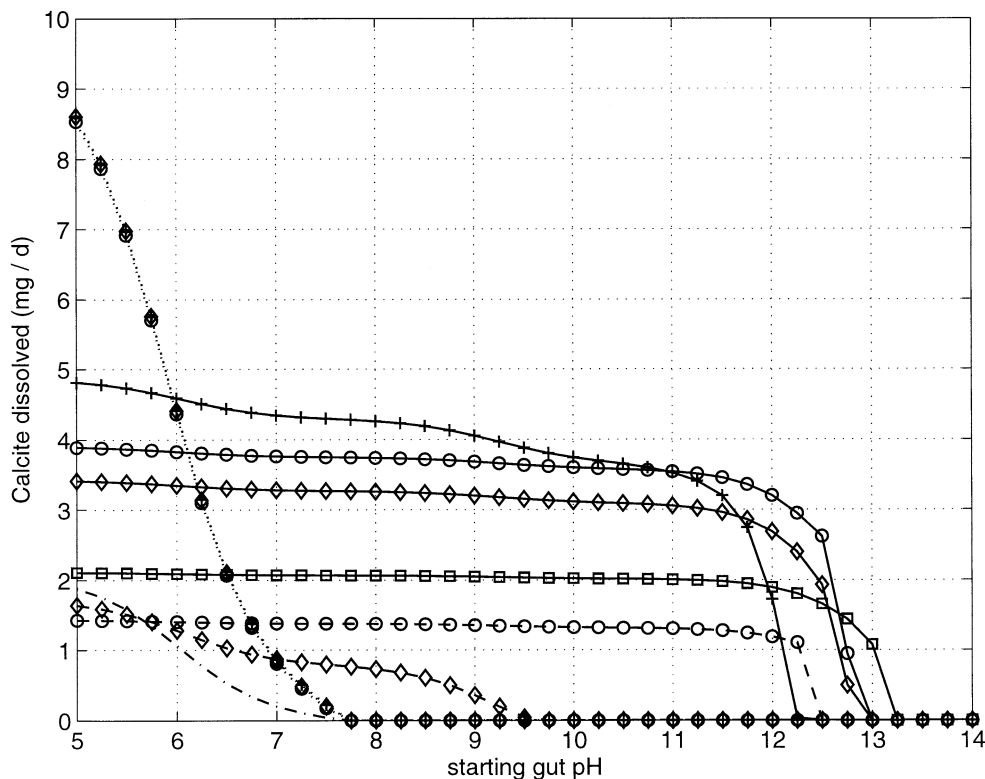


Fig. 4. Influence of starting gut pH on calcite dissolution rate ( $\text{mg d}^{-1}$ ) for 10 hydrographic regimes, differing in depth, OM and calcite content, and OM reactivity (see Table 4): shallow mud ( $\diamond$ ); shallow shell ( $\circ$ ); shallow coralline (+); shallow sewage ( $\square$ ); shelf normal ( $-\diamond-$ ); shelf upwelling ( $-\circ-$ ); continental rise ( $-\bullet-$ ); deep sea clay ( $\cdot\cdot\diamond\cdot\cdot$ ); deep sea diatom ooze ( $\cdot\cdot\circ\cdot\cdot$ ); deep sea foram ooze ( $\cdot\cdot\square\cdot\cdot$ ). Note that all deep sea subregimes practically fall on the same line.

quence of the greater OM reactivity. The finding in Table 4 that dissolution rate increased with increasing OM content for the shelf scenario, while it decreased for the shallow-water cases is readily explained by comparing the location of the respective scenarios relative to the maximum in Figure 9. We found no maximum for the continental rise and deep sea settings within the OM range investigated, as a consequence of diminishing OM reactivity with depth, which tends to shift the maximum to ever larger values of  $\beta$ . While maxima for these depths are theoretically possible for very high values of  $\beta$ , it is unlikely that OM content of most natural sediments exceeds 50%. Furthermore, we observed a relative minimum in calcite dissolution rates at a sediment OM content of  $\sim 10\%$  for the continental rise and deep sea setting,  $\sim 1.5\%$  for the shelf setting and  $\sim 0.3\%$  for the shallow water setting. Dissolution rates increased above and below this minimum, driven by increased microbial respiration in one direction, and driven by increased ingestion in the other. We cannot explain these minima in calcite dissolution by first principles, yet they appear to be recurrent features of the model; they may be attributable to carbonate system effects.

### 3.2.6. Gut Volume

Gut volumes of deposit feeders vary greatly, ranging between  $10^{-2}$  and  $10^4 \text{ mm}^3$  for deposit feeding polychaetes (Penry and Jumars, 1990). Figure 10 shows calcite dissolution

for gut volumes ranging between 10 and  $1000 \text{ mm}^3$  and conditions corresponding to the standard shelf case (Tables 3 and 4). Starting pH was varied from 5 to 7. Because ingestion rate is coupled to gut volume, larger guts ingest and dissolve more calcite than small guts on a mass basis. In terms of percent calcite dissolved, however, the relationship between calcite uptake and calcite dissolution is seen to be less dependent on gut volume.

For performing a global estimate of gut-mediated calcite dissolution, we were interested in how sensitive our results are to the chosen gut volume scale. In other words, we wanted to know whether several small guts dissolve more or less calcite than one large gut of the same total volume. To investigate the allometry of calcite dissolution and gut volume, calcite dissolution rate data were fitted in Figure 11 with an exponential of the form

$$\text{dissolution rate} = \omega_1 V^{\omega_2}, \quad (18)$$

where  $\omega_1$  has been calculated from the choice of  $\omega_2$  and dissolution rates for  $V = 10 \text{ mm}^3$  and four different starting pH conditions. Best fits for the exponent  $\omega_2$  were between 0.85 for a starting pH of 5.5, and 0.96 for a starting pH of 7.7. Thus, at higher gut pH, the allometric exponent approximated linearity, whereas at lower pH it approximated the exponent of 0.77 for ingestion rate, suggesting that calcite delivery becomes more important than respiration rate (i.e. the reaction term) at acidic



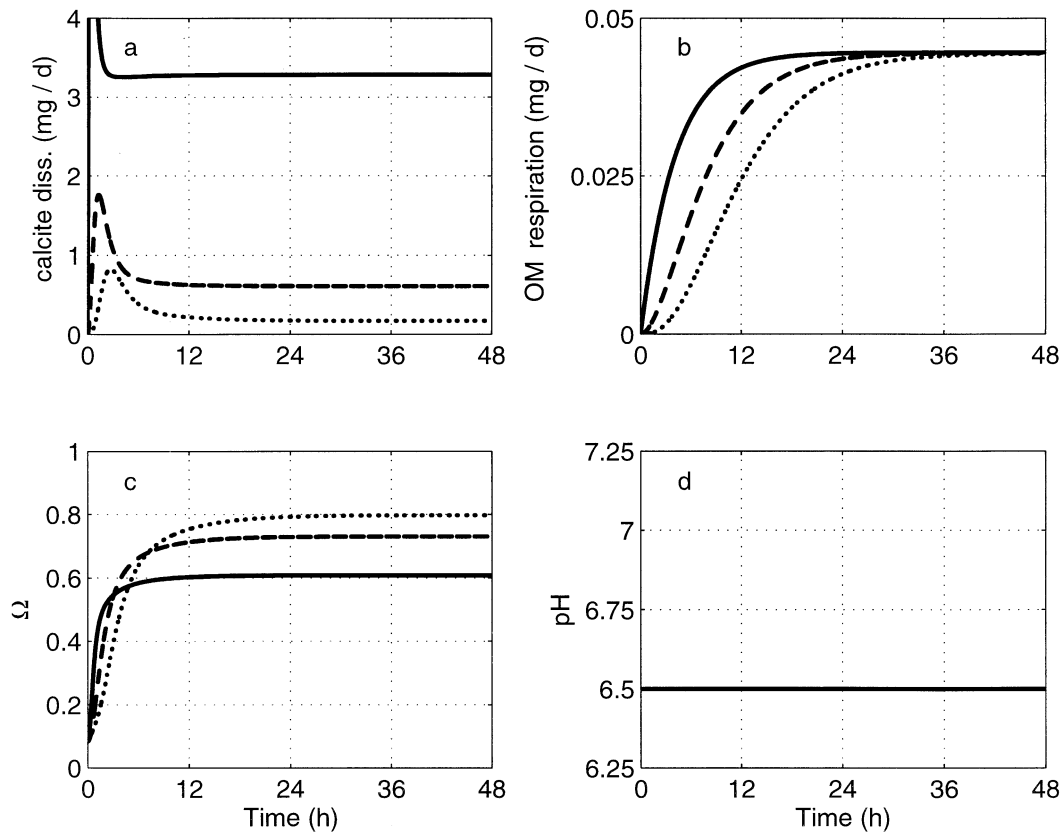


Fig. 5. Dissolution kinetics in a gut with fixed pH (pH 6.5, 1 mL volume, standard shelf conditions), for three gut regions, fore gut (solid line), mid gut (dashed line) and hind gut (dotted line). (a) Calcite dissolution rate. (b) OM respiration rate. (c) Calcite saturation ( $\Omega$ ). (d) Gut pH]. Calcite dissolution in the foregut initially peaks at  $\approx 8.5 \text{ mg d}^{-1}$  (data not shown).

pH, where dissolution rates are likely to be high. The finding that dissolution rate scales more or less linearly with gut volume at neutral pH allows us to disregard scaling effects, which is important for our global estimates described below.

#### 4. DISCUSSION

The important variables controlling calcite dissolution in our model were gut volume, OM content, OM reactivity (decay rate), and starting gut pH. Larger organisms with larger gut volumes ingested more sediment and therefore dissolved a larger absolute amount of calcite. However, the relationship between gut volume and calcite dissolution rate was nonlinear, best described by a power function with an allometric exponent ranging between 0.85–0.96. The combined dissolution rate of several small guts was therefore slightly higher than a single large gut of equivalent volume, becoming increasingly similar for neutral pH. If the scaling exponent were unity, the relationship between calcite dissolution rate and gut volume would be linear, which would allow us to simply model digestive calcite dissolution by deposit feeders as if it occurred in one enormous composite gut volume. The reason why calcite dissolution scaled to gut volume with an allometric exponent greater than that for ingestion rate (0.77; Eqn. 12), is probably due to the fact that only at very low gut pH values (i.e., pH < 5.5) does ingestion rate alone determine calcite dissolution, and the effect of respiration can be neglected. While the universality of the

scaling exponent of 0.77 for ingestion rate may be debatable, it is based on an experimental survey of a large number of polychaete species (Cammen, 1980) and comes very close to the theoretical scaling factor of 0.75 between body mass and many biological metabolic processes (West et al., 1997). It therefore appears reasonable to conclude that calcite dissolution rate scales to gut volume (or individual biomass) with an allometric exponent greater than 0.75 but less than 1, and is close to unity for most guts with near-neutral pH.

Since body-mass-to-gut-volume conversions were based on polychaete meristic data of Penry and Jumars (1990), the model coefficients may be slightly different for other deposit feeding taxa, such as many holothuroids, gastropods and bivalves. However, the general proportionalities and scaling laws are probably universal, namely that ingestion rate is proportional to approximately  $V^{0.75}$  and inversely proportional to the amount of OM. Holothuroids tend to have considerably larger gut volumes than most polychaetes, which would lead to higher individual calcite dissolution rates. Our standard gut volume of 1 mL lies towards the higher end of deposit-feeding polychaete gut volumes (median approximately  $2 \text{ mm}^3$ , as determined by Penry and Jumars, 1990), but is smaller than a typical holothuroid gut volume.

The amount and reactivity of OM are likely to be the most influential biological variables affecting calcite dissolution in guts, since they affect both the delivery of calcite (via ingestion

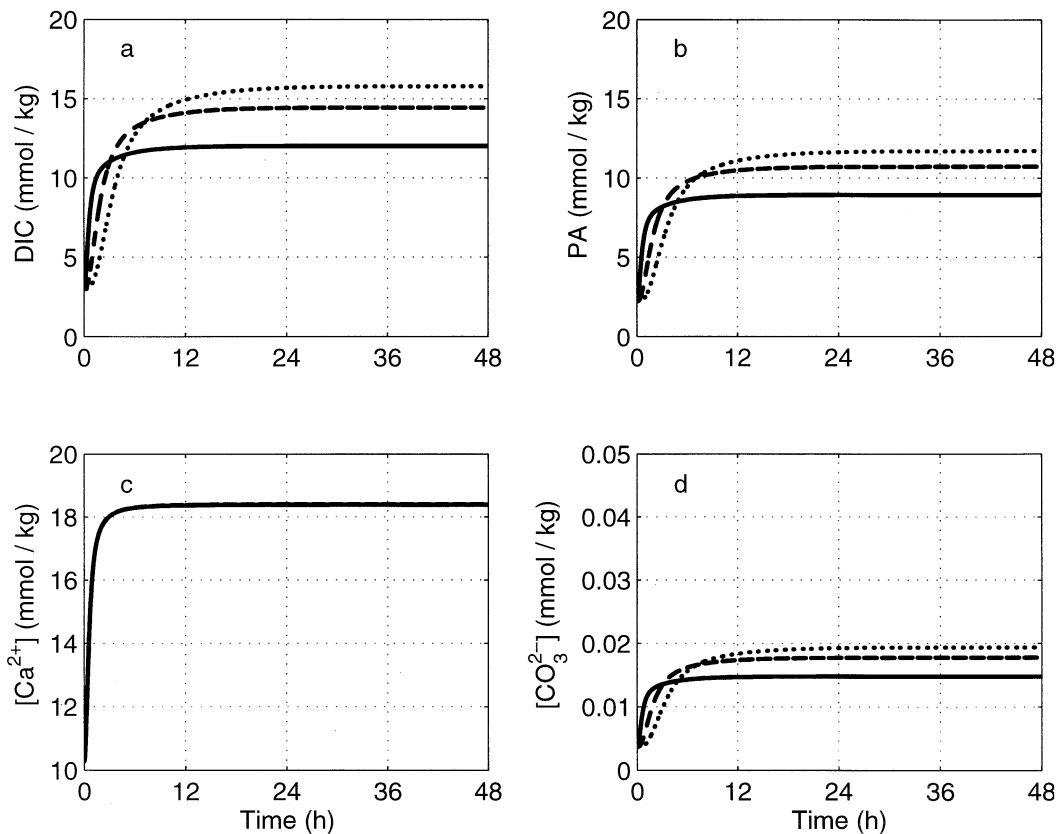


Fig. 6. Fate of dissolved substances in gut with fixed pH (pH 6.5, 1 mL volume, standard shelf conditions), for three gut regions, fore gut (solid line), mid gut (dashed line) and hind gut (dotted line). (a) Dissolved inorganic carbon (DIC). (b) Alkalinity (PA). (c) Dissolved Ca<sup>2+</sup>. (d) Dissolved carbonate.

rate) and the local pH conditions in the gut (via the respiration rate of intestinal microbes). Prolonged gut residence tends to decrease calcite dissolution by increasing calcite saturation. Thus, low sedimentary OM content eliciting high ingestion rates and short gut residence times favors calcite dissolution.

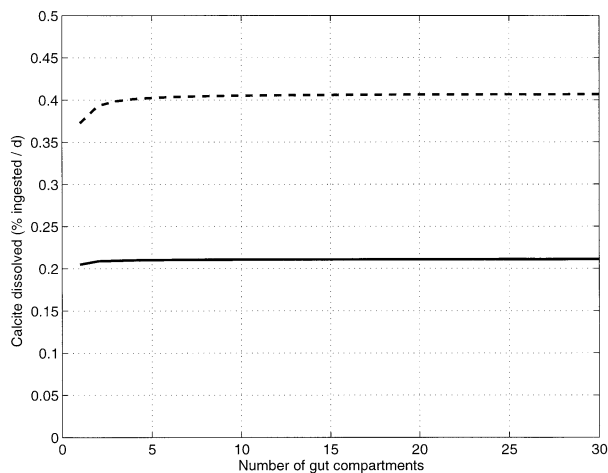


Fig. 7. Influence of number of gut compartments on calcite dissolution efficiency (standard shelf conditions, starting gut pH 6.5), for a small ( $V = 0.01$  mL, solid line) and large gut ( $V = 1$  mL, dashed line).

For this reason, given identical OM reactivity, more calcite may be expected to dissolve in OM-poor shallow water regions, such as coralline sands, compared to OM rich areas (Fig. 4). On the other hand, the more reactive the ingested OM, the more quickly it is respired to CO<sub>2</sub> by gut microbes, promoting dissolution of calcite by counteracting pH rise. Thus, when comparing two sediments with the same OM amount but different OM reactivities, the one with the higher OM reactivity has higher calcite dissolution rates. This is illustrated in Table 4, where the shallow water coralline sediment displayed an approximately four times higher calcite dissolution rate than shelf sediment, even though both had the same assumed OM content of 0.02. The difference was due primarily to the 10 times higher OM decay rate for the shallow water sediment compared to the shelf sediment (Table 3). Deposit feeders in

Table 5. Parameterizations of dissolution kinetics according to Eqn. 10.

Case n	$\kappa$ (d <sup>-1</sup> )	$\eta$ (-)	Reference
1	5	4.5	Keir (1980)
2	1	2.9	Walter and Morse (1985)
3	5	3.0	Morse (1978)
4	0.38	1.0	Hales and Emerson (1997)
5	0.0025	4.5	Aller (1982)

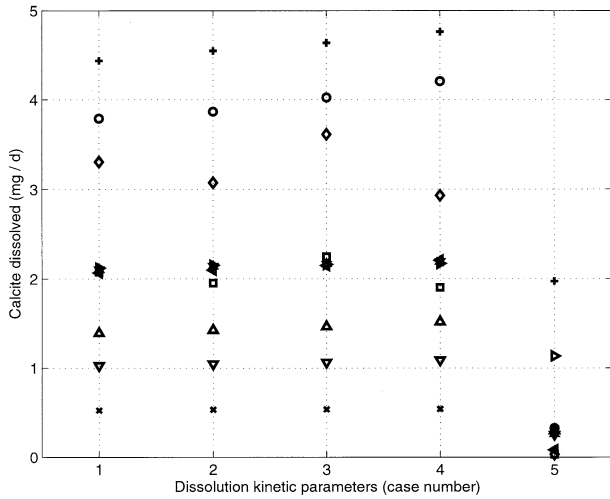


Fig. 8. Influence of dissolution kinetics parameters on calcite dissolution rate ( $\text{mg d}^{-1}$ ), for 10 hydrographic regimes, differing in depth, OM and calcite content, and OM reactivity (see Table 4): shallow mud ( $\diamond$ ) shallow shell ( $\circ$ ), shallow coralline ( $+$ ), shallow sewage ( $\square$ ). Shelf normal ( $\nabla$ ), shelf upwelling ( $\triangle$ ), continental rise ( $\times$ ), deep sea clay ( $\star$ ), deep sea diatom ooze ( $<$ ), deep sea foram ooze ( $\triangleright$ ). For kinetic parameters, see Table 5.

deep-sea sediments have surprisingly similar calcite dissolution rates as their shallow water counterparts as a result of the prodigious feeding rates that result from extremely low OM content.

The key thermodynamic driving force for calcite dissolution is ultimately the pH difference between the gut lumen and the exterior environment. Hereby, we assumed that ingested calcite immediately assumed the pH conditions of the digestive tract and that there was no active physiological pH control on the part of the deposit feeding organism. To counteract the rise in pH due to calcite dissolution, we introduced a reaction term producing carbon dioxide, ascribed to respiration by intestinal microbes and modeled to depend on the amount and the reactivity of OM. Without such a “pH-stat,” the continuous ingestion and dissolution of additional calcite would steadily increase gut pH to a value where no further dissolution occurs. Conversely, in a completely pH-homeostatic gut, where any increases in pH are counteracted by a corresponding influx of protons into the gut maintaining gut pH at a constant value, much greater calcite dissolution rates are possible. Such a situation would involve pH control of the gut lumen by the deposit-feeding organism rather than its gut microbes.

As shown, the starting pH had a significant impact on calcite dissolution rates, with a pH of 7.75 being the “threshold” for gut-mediated dissolution in deep sea and continental rise environments. In shallow regimes, with their high OM content and accordingly intensive microbial respiration, calcite dissolution

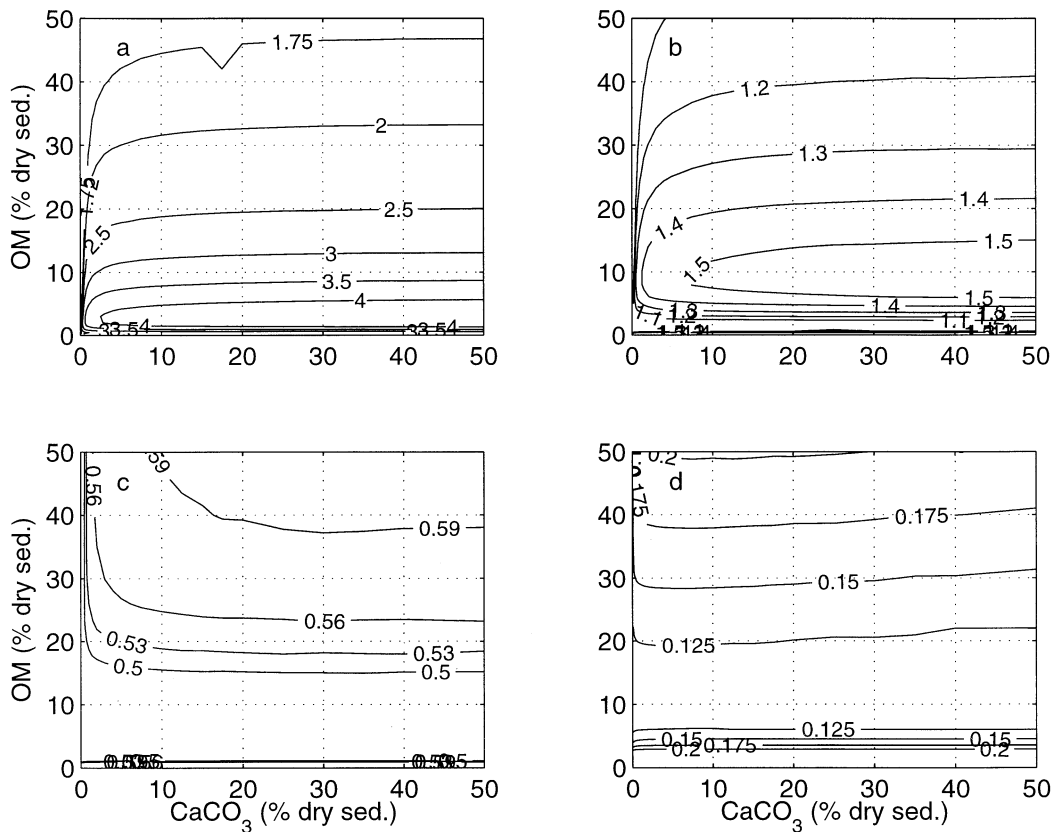


Fig. 9. Calcite dissolution rate ( $\text{mg calcite d}^{-1}$ ) versus sediment calcite and OM content for four oceanographic regimes (differing in OM reactivity): (a) shallow water, (b) shelf, (c) continental rise, and (d) deep sea.

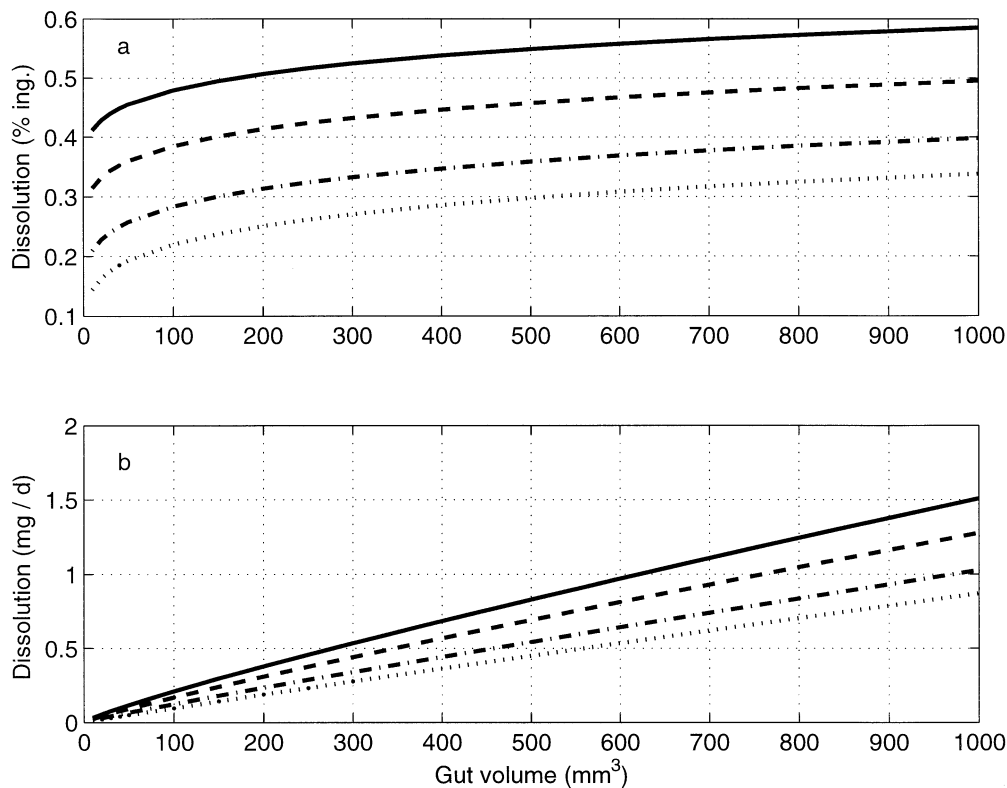


Fig. 10. Calcite dissolution efficiency (% dissolved vs. ingested in a) and dissolution rate ( $\text{mg d}^{-1}$ , b) versus gut volume (standard shelf conditions). Initial pH 5.5 (—), initial pH 6 (---), initial pH 6.5 (— · —), initial pH 7 (····).

was theoretically possible to starting pH values of 13. We realize that this situation is entirely hypothetical because organisms have difficulties with  $\text{NH}_3$  toxicity at alkaline pH. Furthermore, brucite formation, which generally limits pH to less than 9.5 in seawater, has not been considered by the model.

Among the most influential assumptions of our model were the chosen combinations of calcite and OM content and OM reactivity for the different hydrographic regimes. While the magnitude of calcite fraction ( $\alpha$ ) had only limited impact on absolute calcite dissolution rates, the three-order of magnitude variations in  $\beta$  and  $k$  (Tables 3 and 4) resulted in a variation of dissolution rates by up to a factor of  $\sim 9$ . We consider our selection of  $\beta$  and  $k$  for the different hydrographic regimes to be conservative; more extreme conditions are certainly possible in localized environments.

Some limitations of our model are caused because it describes only processes inside the gut and considers only quantity of carbonate dissolved and not its quality. Thus, it remains unclear whether carbonate that is dissolved during gut passage remains dissolved upon defecation, or whether it reprecipitates as soon as intestinal contents rich in dissolved carbonate are expelled into alkaline seawater. Due to kinetic effects (e.g., by concomitantly expelled organic compounds), this newly precipitated carbonate could be of different mineralogy (e.g., aragonite or dolomite), shape or size than the originally ingested material. Thus, it is conceivable, albeit speculative, that deposit feeders affect not only the amount but also the mineralogy of ingested sedimentary carbonate. It should also be remembered that other diagenetic reactions in the gut besides calcite disso-

lution may lead to increased  $\text{Ca}^{2+}$  concentrations or alkalinity, which could increase the ion activity product of dissolved calcium and carbonate and thus depress calcite dissolution.

Without doubt, the greatest uncertainty in estimating calcite dissolution rates is the kinetics of the dissolution process. Carbonate dissolution follows a rate law of the form shown in Eqn. 10, for a wide range of particle sizes and types (Keir, 1980). Experimentally measured values for the rate constant  $\kappa$  vary by over five orders of magnitude. For example,  $\kappa$  measured for fine-grained deep sea foraminifera and coccolith oozes ranged between  $0.3\text{--}30 \text{ d}^{-1}$  (Keir, 1980), while Aller (1982) determined considerably lower values of  $0.00005\text{--}0.0025 \text{ d}^{-1}$  in near-shore sediments consisting primarily of coarse shell hash. Thus, the standard value of  $5 \text{ d}^{-1}$  chosen for the model is admittedly a rather arbitrary compromise that is likely to underestimate dissolution for fine-grained sediments and overestimate dissolution for coarse-grained sediment. A more refined version of our model might therefore distinguish calcite dissolution in separate sediment grain size fractions that differ in calcite reactivity. This could easily be parameterized by different values of  $\kappa$ . It is conceivable that despite favorably low pH conditions and calcite undersaturation ( $\Omega$ ) in the gut, dissolution of calcite is, nonetheless, hindered kinetically. For example, organic coatings on carbonate sediment surfaces have been shown to retard or inhibit carbonate dissolution (Thomas et al., 1993; Müller and Suess, 1977), possibly by slowing down diffusive transport to and from the mineral surface. Since gut fluids are rich in dissolved organic carbon (Mayer et al., 1997), the likelihood of sediment surfaces being coated should

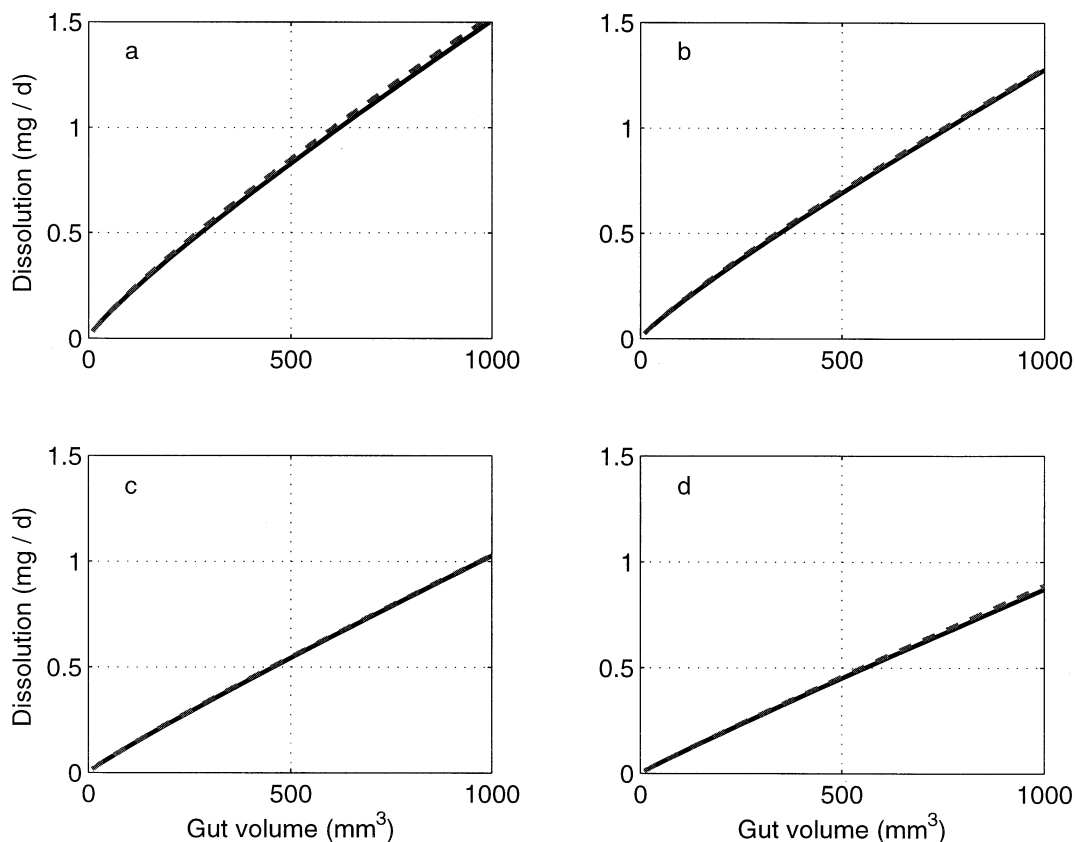


Fig. 11. Dissolution rate versus gut volume, model data (—) and fitted with an exponential model (---) of the form dissolution rate =  $\omega_1 V^{\omega_2}$ . (a) Initial pH 5.5 ( $\omega_2 = 0.85$ ), (b) Initial pH 6 ( $\omega_2 = 0.87$ ), (c) Initial pH 6.5 ( $\omega_2 = 0.91$ ), (d) Initial pH 7 ( $\omega_2 = 0.96$ ).

be high. This could result in an apparent value of  $\kappa$  even lower than the values of Aller (1982). Conversely, organic acids like citrate, malate, pyruvate, which are common metabolic by-products, can associate with free  $\text{Ca}^{2+}$  (Kitano and Hood, 1965) and thereby affect the ion activity product of calcium and carbonate. This may theoretically improve the likelihood of further carbonate dissolution and could favor kinetically slower reactions. However, with a  $\text{Ca}^{2+}$  concentration of approximately 0.01 M, organic ligand concentrations would have to be extremely high to substantially affect free calcium concentration. Finally, release of  $\text{Ca}^{2+}$  from the dissolution of other, noncarbonate minerals, e.g., anhydrite, could theoretically increase the ion activity product of calcium carbonate and thereby reduce the carbonate dissolution rate. The dissolution kinetics of calcium carbonate thus remains an intriguing challenge for further experimental research.

Our model results indicate that the limited published evidence for destruction or corrosion of carbonate particles within guts (Crozier, 1918; Emery et al., 1954; Bonham and Held, 1963; Milliman, 1974) is not at all surprising. While our results show that calcite dissolution in deposit feeder guts is clearly possible for the 5–8 pH range found in the guts of most deposit feeders (Ahrens and Lopez, 2001), the dissolution rates of one to, at most, a few milligrams of calcite per day are likely to be too small to be measurable gravimetrically or by sieve analysis. Since smaller particles generally have higher dissolution kinet-

ics (Morse, 1978; Keir, 1980), it seems likely that these particles experience the bulk of the dissolution. Many very small particles, like fragmented tests of foraminifera, might actually dissolve completely in one event, without evidence of intermediate corrosion stages (Green et al., 1993). Since the total mass and grain size distribution of bulk sediment are likely to change very little due to the dissolution of, at best, a few milligrams carbonate per gut passage, dissolution could pass unnoticed easily. Due to intestinal microbial respiration, significant carbonate dissolution is possible even at pH conditions well above 7, provided there is sufficient OM to fuel microbial respiration. The residence time of sediments within guts of deposit feeders appears to be too short to generate major differences in the dissolution rate and pH between different gut compartments. Thus, a pH difference of greater than 0.2 pH units between adjacent gut compartments is unlikely to be attributable to calcite dissolution. We may therefore conclude that the observed pH increase in deposit feeding annelids, from about pH 5–6 in the stomach to about to pH 8 in the hindgut, as reviewed by Jeuniaux (1969), cannot be attributed to sedimentary carbonate dissolution, but, rather, must be the result of a physiological control by the organism or its gut microbiota. Similarly, the observation of Emery et al. (1954) of a pH increase in a holothurian gut from 6.71–6.93 in the stomach to 7.16–7.60 near the anus, is probably too large to be explained by carbonate dissolution alone. Apparently, as with terrestrial animals,

Table 6. Global estimate of gut-mediated benthic calcite dissolution.

Depth range (m)	0–20	20–200	200–1000	1000–5000	Sum	Reference
Ocean surface (%)	0.75	6.7	4.4	65.5	77.4	Menard and Smith (1966)
Deposit feeder biomass ( $\text{g m}^{-2}$ )	50	10	1	0.1		Zenkevitch et al. (1971) <sup>a</sup>
Gut volume density ( $\text{mL m}^{-2}$ )	14.2	2.84	0.28	0.03		This study
Calcite dissolution rate in guts ( $\text{mg d}^{-1} \text{mL}^{-1}$ )	3	0.5	1	2		This study
Average dissolution rate ( $\text{mg d}^{-1} \text{m}^{-2}$ )	42.6	1.4	0.28	0.06		This study
Global calcite dissolution rate ( $10^{10} \text{ mol Ca}^{-1}$ )	42.2	12.7	1.7	4.9	61.4	This study
Annual dissolution rate (%) <sup>b</sup>	3.25	0.97	0.13	0.38	4.72	This study

<sup>a</sup> Estimated assuming 50% of benthic biomass to be deposit feeders.

<sup>b</sup> Based on total annual benthic carbonate dissolution of  $13 \cdot 10^{12} \text{ mol Ca}^{-1}$ , as estimated by Milliman et al. (1999).

deposit feeders that possess several gut compartments with measurably different pH conditions must derive some digestive benefit from this, which is likely to be related to an optimization of different enzymatic processes.

A quantitative method to detect carbonate dissolution reliably would have to be capable of measuring changes of approximately 1 mg carbonate or 0.01 mmol alkalinity. The alkalinity differences of 0.1–0.4 mEqv (0.05–0.2 mmol/L) measured by Hammond (1981) thus seem realistic, although somewhat higher, which may be explained by the fact that Hammond's data were obtained for large-bodied holothuroids. Other suitable methods to detect carbonate corrosion would be to quantify etching of small carbonate particles, such as calcareous foraminifera tests, using electron microscopy, as performed by Mageau and Walker (1976). However, since small particles could dissolve completely when they do dissolve, and, therefore, leave no trace of their history, this approach may prove to be futile nonetheless. Furthermore, an optical method would probably be only semiquantitative. Another alternative to quantify carbonate dissolution would be to subject radiolabeled carbonate particles to gut fluids and monitor the concentration change of the tracer ions in the gut fluid. The sensitivity of a radiometric method should be sufficient to detect dissolution in the nanomolar concentration range. Finally, an accurate description of the spatial pH distribution in a deposit feeder animal digesting carbonate might be valuable. An *in vivo* microfluorimetric approach may be amenable to this purpose (Pond et al., 1995; Ahrens and Lopez, 2001).

Using our model results, we now attempt to estimate the contribution of deposit feeder digestion to the global calcite dissolution budget. For this, we take typical calcite dissolution rates generated by our model for different water depths, and assume a depth-dependent deposit feeder biomass. Seafloor provinces below the lysocline (i.e. below 5000 m) are disregarded, as are variations in calcite dissolution rates resulting from gut volume allometry (i.e., we assume that all deposit feeders have a gut volume of 1 mL). Approximate deposit feeder biomass was estimated from benthic biomass values from the literature, assuming that 50% of the benthic biomass is due to deposit feeders. Biomass and corresponding gut volumes are summarized in Table 6. The calcite dissolution flux for each depth horizon was calculated by multiplying typical model estimates for calcite dissolution by the composite gut volume present per unit area ("gut volume-density"). By further

multiplying the carbonate dissolution flux of each depth horizon by its proportion of the world seafloor area ( $3.62 \cdot 10^8 \text{ km}^2$ , Dietrich et al., 1975), we generate global estimates of carbonate dissolution (in  $\text{mol Ca}^{-1}$ ) for each hypsographic region. As shown in Table 6, we calculate an annual gut-mediated carbonate dissolution flux of  $0.61 \cdot 10^{12} \text{ mol Ca}^{-1}$  for the entire seafloor shallower than 5000 m. This amounts to approximately 5% of the annual benthic carbonate dissolution of  $13 \cdot 10^{12} \text{ mol Ca}^{-1}$  (Milliman et al., 1999), and corresponds to an average gut-mediated dissolution rate of approximately  $0.5 \text{ mg m}^{-2} \text{ d}^{-1}$ . In this estimate, more than two thirds of the gut-mediated dissolution rate is due to benthos living at depths of 0–20 meters, which comprises less than 1% of the world seafloor area. Gut-mediated dissolution on shelf sediments (20–200 m) contributes approximately 1% of the global benthic carbonate dissolution, whereas seafloor regions below 200 m, despite their vast areal extent, contribute less than 1%. The low carbonate dissolution flux with increasing water depth is primarily a result of the exponentially diminishing benthic biomass. While Table 6 demonstrates that the role of benthic deposit feeder digestion in global carbonate dissolution budgets greatly depends on the assumed deposit feeder abundances, we consider these values to be conservative. Assumed dissolution rates are conservative as well, since we base our estimate on a moderate gut pH of 6.5, and consider calcite dissolution only. For example, aragonite is more soluble than calcite (Mucci et al., 1989) and comprises 30–50% of the global sediment carbonate content (Berner, 1977). Aller (1982) estimated calcite dissolution flux in nearshore shallow water environments to be  $10\text{--}50 \text{ g m}^{-2} \text{ a}^{-1}$ . Our calculated shallow water dissolution rate of  $42 \text{ mg m}^{-2} \text{ d}^{-1}$  ( $15.5 \text{ g m}^{-2} \text{ a}^{-1}$ ) thus amounts to approximately 30–155% of this flux. Our global estimate for shallow water dissolution agrees within a factor of 2 with Hammond's (1981) estimate for a Jamaican coral reef flat, where three prevailing species of deposit-feeding holothurians were estimated to dissolve  $11 \text{ g m}^{-2} \text{ a}^{-1}$ , or 2% of the annual carbonate fixation of the reef. Our deep sea estimate of  $0.6 \text{ mg m}^{-2} \text{ d}^{-1}$  amounts to less than 1% of the benthic carbonate dissolution flux of  $5\text{--}68 \text{ mg m}^{-2} \text{ d}^{-1}$  by Martin and Sayles (1996) and Hales and Emerson (1997) for several stations on the Ceara Rise, western tropical Atlantic (depth: 3300–4700 m). At these depths, bottom water undersaturation undoubtedly becomes the prevailing driver of carbonate dissolution. Nonetheless,  $\text{CO}_2$  produced by metabolic processes within the sed-

iment continues to be important, further supplementing hydrostatic pressure induced undersaturation. This has been demonstrated by fitting reaction-diffusion models to pore water data (Hales and Emerson, 1997). However, it is probable that the prevailing source of metabolic CO<sub>2</sub> in deep sea sediments is predominantly “free-living” sediment microbes rather than gut microbes or their deposit feeding hosts. Ultimately, whether occurring in animal guts or in sediments, it is microbial respiration that drives biologically-mediated carbonate dissolution.

Finally, it should be noted that our model assumes seasonally stable benthic abundance and activity patterns. Given the predominant role of nearshore sediments for carbonate dissolution, it would be interesting to investigate the seasonality of gut-mediated carbonate dissolution. As abundance and activity in nearshore benthic populations can fluctuate considerably in temperate and polar regions, as a result of lower temperatures and more refractory food input, it is well possible that gut-mediated carbonate dissolution oscillates in a similar fashion.

## 5. CONCLUSION

The scarcity of published evidence for CaCO<sub>3</sub> dissolution in guts of deposit feeders may be explained by the minute, milligram amounts of carbonate that dissolve per gut passage and the methodological inadequacy of most previous studies in measuring these small changes. Alternatively, while clearly being thermodynamically possible, carbonate dissolution in guts may be hindered kinetically, although currently there exists no evidence for this.

Sensitivity analysis shows that variations of OM quantity and quality, encompassing the whole spectrum of marine sediments, affect dissolution rates by generally less than one order of magnitude. Carbonate dissolution rates should therefore be primarily dependent on deposit feeder abundances. Our calculated steady-state gut pH of ~ 5.5–7.5 for calcite-ingesting deposit feeders, covering a wide range of sedimentary conditions, agrees favorably with the range of gut pH measured in field-collected animals. Our model suggests that shallow water deposit feeding animals, both individually and in numbers, dissolve more calcite than deep sea deposit feeders, and, as a result of greater microbial respiration, have slightly more acidic guts than deep sea deposit feeders. This predicted difference in CaCO<sub>3</sub> dissolution rate and gut pH conditions between deep sea and shallow water deposit feeders would be an interesting hypothesis to test in the field.

*Acknowledgments*—We thank Robert H. Byrne and two anonymous reviewers, whose comments greatly improved the manuscript.

*Associate editor:* R. H. Byrne

## REFERENCES

- Ahrens M. J. and Lopez G. R. (2001) In vivo characterization of the gut chemistry of small deposit-feeding polychaetes. In *Organism-Sediment Interactions* (eds. J. Y. Aller, S. A. Woodin, and R. C. Aller), pp. 349–368. University of South Carolina Press.
- Aller R. C. (1982) Carbonate dissolution in nearshore terrigenous muds: The role of physical and biological reworking. *J. Geol.*, **90**, 79–95.
- Berner R. A. (1977) Sedimentation and dissolution of pteropods in the ocean. In *The Fate of Fossil Fuel CO<sub>2</sub> in the Oceans*, Vol. 6 of *Marine Science* (eds. N. R. Anderson and A. Malankoff). pp. 243–259. Plenum Press.
- Berner R. A. (1980) *Early Diagenesis—A Theoretical Approach*. Princeton University Press.
- Bezrukov P. L., Emelyanov E. M., Lisitsyn A. P., and Romankevich E. A. (1977) Organic carbon in the upper sediment layer of the worlds oceans. *Okeanologiya* **17**, 850–854.
- Bonham K. and Held E. E. (1963) Ecological observations on the sea cucumbers *Holothura atra* and *Holothuria leucospilata* at Rongelap Atoll. *Pac. Sci.* **17**, 305–314.
- Cai W.-J., Reimers C. E., and Shaw T. (1995) Microelectrode studies of organic carbon degradation and calcite dissolution at a California Continental rise site. *Geochim. Cosmochim. Acta* **59**, 497–511.
- Cammen L. M. (1980) Ingestion rate, an empirical model for aquatic deposit feeders and detritivores. *Oecologia* **44**, 303–310.
- Crozier W. J. (1918) The amount of bottom material ingested by holothurians (Stichopus). *J. Exp. Zool.* **26**, 379–389.
- Dietrich G., Kalle K., Krauss W., and Siedler G. (1975) *Allgemeine Meereskunde*. Gebrüder Bornträger, Berlin.
- DOE (1994) Handbook of methods for the analysis of the various parameters of the carbon dioxide system in sea water. Version 2. ORNL/CDIAC-74. Available at: <http://andrew.ucsd.edu/co2qc/handbook.html>.
- Emery K. O. (1962) *Marine Geology of Guam*, volume 403 of Professional Paper 403. U.S. Geological Survey.
- Emery K. O., Tracey J. I. Jr., and Ladd H. S. (1954) *Geology of Bikini and Nearby Atolls*. Professional Paper 260. U.S. Geological Survey.
- Fisher J. B. and Matisoff G. (1981) High resolution vertical profiles of pH in recent sediments. *Hydrobiologia* **79**, 277–284.
- Gorham E. (1960) The pH of fresh soils and soil solutions. *Ecology* **41**, 563–563.
- Green M. A., Aller R. C., and Aller J. Y. (1993) Carbonate dissolution and temporal abundances of foraminifera in long island sound sediments. *Limnol. Oceanogr.* **38**, 331–345.
- Grim R. E. (1962) *Applied Clay Mineralogy*. McGraw-Hill.
- Hales B. and Emerson S. (1997) Evidence in support of first-order dissolution kinetics of calcite in seawater. *Earth Planet. Sci. Lett.* **148**, 317–327.
- Hammond L. S. (1981) An analysis of grain size modification in biogenic carbonate sediments by deposit-feeding holothurians and echinoids (Echinodermata). *Limnol. Oceanogr.* **26**, 898–906.
- Jansen H. and Wolf-Gladrow D. A. (2001) Carbonate dissolution in copepod guts: A numerical model. *Mar. Ecol. Prog. Ser.* **221**, 199–207.
- Jeuniaux C. (1969) Nutrition and digestion. In *Chemical Ecology*, Vol. 4 (eds. M. Florkin and B. R. Scheer), pp. 69–91. Academic Press.
- Keir R. S. (1980) The dissolution kinetics of biogenic calcium carbonates in seawater. *Geochim. Cosmochim. Acta* **44**, 241–252.
- Kitano Y. and Hood J. D. W. (1965) The influence of organic material on the polymorphic crystallization of calcium carbonate. *Geochim. Cosmochim. Acta* **29**, 29–41.
- Martin W. R. and Sayles F. L. (1996) CaCO<sub>3</sub> dissolution in sediments of the Ceara Rise, western equatorial Atlantic. *Geochim. Cosmochim. Acta* **60**, 243–263.
- Mageau N. C. and Walker D. A. (1976) Effects of ingestion on foraminifera by larger invertebrates. *Marit. Sediment. Pec. Publ.* **1**, 89–105.
- Mayer L. M., Schick L. L., Self R. F. L., Jumars P. A., Findlay R. H., Chen Z., and Sampson S. (1997) Digestive environments of benthic macroinvertebrate guts: Enzymes, surfactants and dissolved organic matter. *J. Mar. Res.* **55**, 785–812.
- Mayor A. G. (1924) Causes which produce stable conditions in the depth of the floors of pacific fringing reef-flats. *Carnegie Inst. Wash. Publ.* **340**, 27–36.
- Menard H. W. and Smith S. M. (1966) Hypsometry of ocean basin provinces. *J. Geophys. Res.* **71**, 4305–4325.
- Middelburg J. J. (1989) A simple rate model for organic matter decomposition in marine sediments. *Geochim. Cosmochim. Acta* **53**, 1577–1588.

- Millero F. J. (1995) Thermodynamics of the carbon dioxide system in the oceans. *Geochim. Cosmochim. Acta* **59**, 661–677.
- Milliman J. D. (1974) *Marine Carbonates*. Springer-Verlag.
- Milliman J. D., Troy P. J., Balch W. M., Adams A. K., Li Y.-H., and Mackenzie F. T. (1999) Biologically mediated dissolution of calcium carbonate above the chemical lysocline? *Deep-Sea Res. I* **46**, 1653–1669.
- Morse J. W. (1978) Dissolution kinetics of calcium carbonate in sea water: VI. The near-equilibrium dissolution kinetics of calcium carbonate-rich deep sea sediments. *Am. J. Sci.* **278**, 344–353.
- Morse J. W. and Mackenzie F. T. (1990) *Geochemistry of Sedimentary Carbonates*. Elsevier.
- Mucci A., Canuel R., and Zhong S. (1989) The solubility of calcite and aragonite in sulfate-free seawater and the seeded growth kinetics and composition of the precipitates at 25°C. *Chem. Geol.* **74**, 309–320.
- Müller P. J. and Suess E. (1977) Interaction of organic compounds with calcium carbonate—III. Amino acid composition of sorbed layers. *Geochim. Cosmochim. Acta* **41**, 941–949.
- Penry D. L. and Jumars P. A. (1987) Modeling animal guts as chemical reactors. *Am. Nat.* **129**, 69–96.
- Penry D. L. and Jumars P. A. (1990) Gut architecture, digestive constraints and feeding ecology of deposit-feeding and carnivorous polychaetes. *Oecologia* **82**, 1–11.
- Plante C. J., Jumars P. A., and Baross J. A. (1990) Digestive associations between marine detritivores and bacteria. *Ann. Rev. Ecol. System.* **21**, 93–127.
- Plante C. and Jumars P. (1992) The microbial environment of marine deposit feeder guts characterized via microelectrodes. *Microb. Ecol.* **23**, 257–277.
- Pond D. W., Harris R. P. and Brownlee C. (1995) A microinjection technique using a pH-sensitive dye to determine the gut pH of *Calanus helgolandicus*. *Mar. Biol.* **123**, 75–79.
- Reimers C. E. (1982) Organic matter in anoxic sediments off central Peru: Relations of porosity, microbial decomposition and deformation properties. *Mar. Geol.* **46**, 175–197.
- Sayles F. L. (1980) The solubility of CaCO<sub>3</sub> in seawater at 2°C based upon in-situ sampled pore water composition. *Mar. Chem.* **9**, 223–235.
- Thomas M. M., Clouse J. A., and Longo J. M. (1993) Adsorption of organic-compounds on carbonate minerals. 3. Influence on dissolution rate. *Chem. Geol.* **109**, 227–237.
- Walter L. M. and Morse J. W. (1985) The dissolution kinetics of shallow marine carbonates in seawater: A laboratory study. *Geochim. Cosmochim. Acta* **49**, 1503–1513.
- Webb K. L., DuPaul W. D., and Elia C. F. D. (1977) Biomass and nutrient flux measurements on *Holothuria atra* populations on windward reef flats at Enewetak, Marshall Islands. In *Proceedings of the Third International Coral Reef Symposium*, pp. 409–415. Rosenstiel School of Marine and Atmospheric Science, University of Miami.
- West G. B., Brown J. H., and Enquist J. B. (1997) A general model for the origin of allometric scaling laws in biology. *Science* **276**, 122–126.
- Withers P. C. (1992) *Comparative Animal Physiology*. Saunders College Publishing.
- Yamanouti T. (1939) Ecological and physiological studies on holothurians in the coral reefs of Palao Islands. *Palao Trop. Biol. Station Stud.* **1**, 603–636.
- Yingst J. Y. (1974) The utilization of organic detritus and associated microorganisms by *Parastichopus parvimensis*, a benthic deposit-feeding holothurian. Ph.D. thesis. University of Southern California.
- Young J. R. (1994) Functions of coccoliths. In *Coccolithophores* (ed. A. Winter), pp. 63–82. Cambridge University Press.
- Zeebe R. E. and Wolf-Gladrow D. (2001) *CO<sub>2</sub> in Seawater: Equilibrium, Kinetics, Isotopes*. Elsevier.
- Zenkevitch L. A., Filatova A., Belyaev G. M., and Suetova I. A. (1971) Quantitative distribution of zoobenthos in the world ocean. *Bull. Moskauer Gen. Nat. Abt. Biol.*